Clays and Clay Minerals (2025), **73**, e12, 1–10
doi:10.1017/cmn.2025.1

Original Paper

Engineering performance and microstructural behavior of kaolin treated with nano-materials

Swapna Thomas[1], S. Chandrakaran[2] and N. Sankar[2]

[1]Department of Civil Engineering, Saintgits College of Engineering, Kottayam-686532, India and [2]Department of Civil Engineering, National Institute of Technology, Calicut-673601, India

Abstract

This research tackles the challenge of enhancing the engineering properties of kaolinite-rich clay through innovative and sustainable treatment approaches. The main aim was to investigate the effects of nano-materials such as calcium carbonate and silica on the plasticity, strength, compressibility, and microstructural behavior of kaolin. The experimental process involved blending kaolin with varying concentrations (0.5–2% by dry weight) of calcium carbonate and silica. Standard laboratory tests, such as Atterberg limits, unconfined compressive strength (UCS), and one-dimensional consolidation tests, were performed to evaluate changes in plasticity, mechanical strength, and compressibility. Microstructural analyses using X-ray diffraction (XRD), scanning electron microscopy (SEM), Fourier-transform infrared spectroscopy (FTIR), and Brunauer-Emmett-Teller (BET) provided insights into the structural and surface modifications of the treated clay. The findings demonstrated a notable reduction in the plasticity index of kaolin as the nano-material content increased, with the optimal dosage identified at ~1% for both nano-materials. At this dosage, the UCS of the treated clay increased threefold, attributed to the formation of a nano-crystalline gel and improved particle interactions. Consolidation tests revealed a significant decrease in the compression index, while the hydraulic conductivity remained similar to that of untreated kaolin. Microstructural analysis confirmed the development of an aggregated-flocculated structure, enhanced pore connectivity, and increased surface area in the clay nano-composite. In summary, the incorporation of calcium carbonate and silica particles significantly enhanced the engineering characteristics of kaolinite-rich clay, highlighting their promise as sustainable alternatives for clay improvement. These results pave the way for broader applications of nano-materials in geotechnical engineering.

Keywords: calcium carbonate; compressibility; kaolin; silica; strength

(Received: 27 February 2024; revised: 22 November 2024; accepted: 08 January 2025)

Introduction

Kaolinite is one of the major mineral constituents found extensively in soil and rock formations worldwide. Kaolinite is a 1:1 dioctahedral phyllosilicate formed by the superposition of silicon tetrahedral sheets and aluminum octahedral sheets (Harman and Fraulini, 1940; Cheng et al., 2012). It is characterized by a relatively low cation exchange capacity and shrink-swell capacity (Mitchell and Soga, 1994). The sorption activity of the kaolinite structure mostly occurs at the external and basal edge surfaces due to the strong hydrogen bonding that exists between the silica and alumina sheets within the inner plane (Miranda-Trevino and Coles, 2003). The ion exchange, potentially facilitated by hydroxyl edge sites and exposed hydroxyl planes, is influenced strongly by particle size and soil pH levels (Ma and Eggleton, 1999). The high value of soil pH could enhance the release of hydrogen ions from the kaolinite mineral, leading to an increase in its cation exchange capacity.

This research focuses on exploring the influence of nano-materials, specifically calcium carbonate and silica, on the engineering properties and microstructural behavior of clay, where kaolinite is the dominant mineral constituent. Traditional soil stabilization methods often rely on cement or lime, which, while effective, can have significant environmental and economic drawbacks. In response to these limitations, this study explores innovative and sustainable treatment methods by incorporating nano-materials, specifically calcium carbonate and silica particles. These materials, due to their large surface area and reactivity, have the potential to enhance the microstructural and macroscopic properties of kaolin significantly. The research investigates the effects of these materials on critical soil parameters, including plasticity, strength, compressibility, and microstructural behavior. By studying these interactions systematically, the study aims to develop a more sustainable and effective approach for the treatment and stabilization of kaolinite-rich clay, ultimately contributing to the advancement of sustainable geotechnical practices.

Corresponding author: Swapna Thomas; Emails: swapnarenjit@gmail.com; swapna_p190097ce@nitc.ac.in

Cite this article: Thomas S., Chandrakaran S., & Sankar N. (2025). Engineering performance and microstructural behavior of kaolin treated with nano-materials. *Clays and Clay Minerals* **73**, e12, 1–10. https://doi.org/10.1017/cmn.2025.1

© The Author(s), 2025. Published by Cambridge University Press on behalf of The Clay Minerals Society.

The rapid advancement in nano-science has prompted many geotechnical researchers to explore the possible application of nano-materials in soil treatment. Various types of nano-materials, such as silica, alumina, calcium carbonate, and graphene, have been applied to various soil types to investigate their impact on geotechnical properties (Kannan and Sujatha, 2021; Thomas et al., 2022). The stabilization of dispersive clay and strengthening of cement-blend soft clay having shear strength less than 25 kPa were achieved with the addition of silica (Fattahi Masrour et al., 2021; Thomas and Rangaswamy, 2020). The incorporation of 1% silica modified the clay to be non-dispersive by enhancing the cohesion and internal friction angle. Silica served as an active catalyst for the pozzolanic reactions in cement-blended soft clay. The incorporation of calcium particles modified the geotechnical properties of clay obtained from a paddy field, cement-stabilized marine soil, and clayey sand (Meng et al., 2017; Mohammadi et al., 2022; Thomas et al., 2023). The unconfined compressive strength of paddy clay was increased significantly due to the formation of calcium silicate hydrate gel with the addition of 1.5% $CaCO_3$. Similarly, $CaCO_3$ improved the compressive strength of cement-stabilized marine soil at an early stage, due to its ability to fill the pore spaces in the clay and nucleation effects. The clayey sand exhibited more brittle behavior and enhanced soil cementation with the addition of $CaCO_3$. The interconnection between clay particles was enhanced by the addition of graphene oxide nano-particles in cement-treated silty soil (Naseri et al., 2016; Zhou et al., 2017; Aziz et al., 2023). In addition, the treatment of clay with silica and alumina along with cement has improved the soaked and unsoaked California Bearing Ratio (CBR) strengths (Karimiazar et al., 2022). The greatest CBR strength was achieved with the combination of 1% silica and 3% cement, while the lowest free swell potential was attained with the combined use of 3% cement and 1% alumina.

The addition of alumina significantly improved the shear strength of kaolinite, commonly known as Iran porcelain soil (Parsaei et al., 2023). The plasticity index decreased, the internal friction angle increased, and unconfined compressive strength reached its peak value with the addition of 4% alumina in kaolinite. Similarly, an increase in unconfined compressive strength and Young's modulus was observed when kaolin was treated with an optimal percentage of ~4% silica (Moayed and Rahmani, 2017). However, studies on the effect of nano-materials on the geotechnical performance of kaolinite-dominant clays have been limited. More research is thus needed in this field to leverage the unique properties of nano-materials to enhance the characteristics of the clays. Existing literature suggests that silica and $CaCO_3$ are the two primary nano-materials used for clay-based experiments.

The treatment using nano-materials is typically influenced by the pH value, cation exchange capacity, and the type of dominant mineral present in the clay. A comprehensive understanding of the influence of nano-materials on kaolin, therefore, is essential, as kaolinite is a prevalent mineral in various soils. The primary objective of the present work was to determine the fundamental behavioral changes in kaolin with the incorporation of nano-scale materials. This work focused mainly on evaluating the engineering behavior and physio-chemical characteristics of kaolin when mixed with nano-materials such as calcium carbonate and silica. Both silica and calcium carbonate can be considered green materials due to their potential to reduce environmental impact through enhanced material properties, energy efficiency, and utilization of natural or waste-derived resources. Silica can be derived from natural sources such as sand or agricultural waste (e.g. rice husk ash), making it a potentially sustainable option. Calcium carbonate can be produced from abundant natural resources such as limestone, and some production techniques also utilize waste products from other industries, promoting recycling and waste reduction efforts. The present study also aimed to assess the microstructural modifications in kaolin, mainly in terms of crystalline structure and surface morphology after treatment.

Materials and methods

Kaolin

The clay used in this study was kaolin (KC), commonly referred to as China clay, purchased commercially from the AksharChem store in Mumbai, India. It consisted mainly of kaolinite along with some illite and quartz, as ascertained by X-ray diffraction (XRD; Fig. 1). The clay was soft, with a plastic nature, and white in color. The grain-size distribution curve (Fig. 2) determined through hydrometer analysis showed that the clay-sized fraction (<2 μm) in the kaolin was ~43%. The soil pH was measured using a pH meter as 7.8, and the specific gravity was obtained as 2.57 g cm^{-3} from the density bottle test conducted in the laboratory. The clay had a liquid limit (LL) of 44% and a plasticity index (PI) of 16%, which falls in the intermediate plasticity (CI) category according to the IS plasticity chart (IS 1498, 1970). The shrinkage limit (SL) of the kaolin was 27%, its maximum unit weight was 13.9 kN m^{-3}, and its optimum moisture content was 29%. The chemical composition of the kaolin, as obtained by X-ray fluorescence (XRF) analysis, is provided in Table 1.

Nano-materials

Two types of commercially purchased nano-materials, namely calcium carbonate and silica, were utilized in this study. The calcium carbonate nano-particles were hexagonally shaped, with an average particle size ranging from 70 to 100 nm, whereas the silica particles were spherical, with particle sizes varying between 30 and 50 nm. Both types of nano-particles presented a white, powdery appearance. The particle densities of calcium carbonate and silica were 2.7 and 2.5 g cm^{-3}, respectively. The purity of calcium carbonate was 99.9%, while that of silica was 99.5%. Calcium carbonate was provided by Nanoshel, Intelligent Materials Pvt. Ltd, Gujarat, India, and silica was sourced from Nano Research Lab, Jamshedpur, India (Thomas et al., 2023; Thomas et al., 2024).

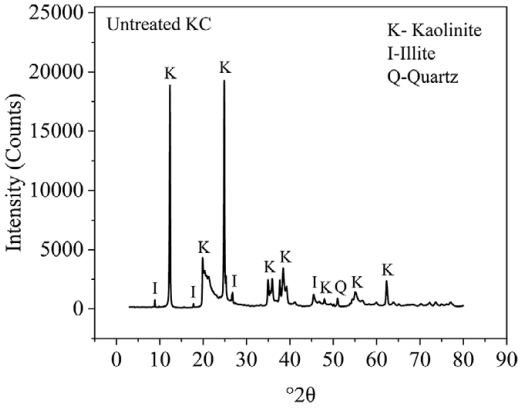


Figure 1. XRD pattern of untreated kaolin (KC).

https://doi.org/10.1017/cmn.2025.1 Published online by Cambridge University Press

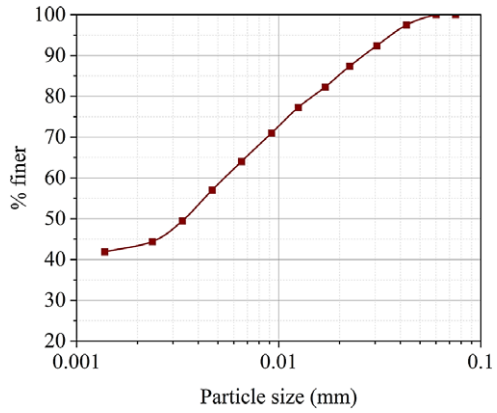


Figure 2. Grain-size distribution curve of kaolin.

Table 1. Chemical composition of kaolin

Oxide	Weight (%)
SiO_2	48.79
Al_2O_3	48.16
Fe_2O_3	1.526
Ti	1.148
CaO	0.141
K_2O	0.077
MgO	0.063
P_2O_5	0.062

Nano-treatment procedure

The test specimens were prepared by adding varying concentrations of nano-materials (calcium carbonate and silica) to the specified quantity of kaolin. The nano-dosages were varied at 0.5, 1, 1.5, and 2% per dry unit weight of the clay. As nano-materials in powder form tend to agglomerate, they were dispersed in a deflocculating medium at a ratio of 1 g of nano-powder to 5 mL of the medium (the ratio was fixed after many trials). The deflocculating medium was obtained by mixing 33 g of sodium hexametaphosphate and 7 g of sodium carbonate in 1000 mL of distilled water. The required dose of nano-materials, dispersed well in the deflocculating medium, was mixed with the weighed quantity of kaolin and the optimal amount of water (29%). Hand mixing was done until a uniform mixture was obtained. After thorough blending, the clay-nano-particle mixture was compacted to its maximum dry unit weight (13.9 kN m^{-3}) in a split mold of size 38 mm×76 mm to obtain the clay nano-composite samples. The optimum water content and maximum dry unit weight were obtained by conducting the Standard Proctor compaction test on kaolin (IS 2720 (Part 7), 1997). The specimens were then kept for curing for a period of 7 days, then extended to 28 days. Curing is the process of storing the test samples in a desiccator for a specified duration to prevent moisture loss from the sample and allow sufficient time for chemical reactions between the clay minerals and additives to occur. The durations were chosen to evaluate strength development within 1 week (early stage) and to determine whether the chemical reactions were dependent on time over a 28-day period (later stage).

Methodology

Atterberg's limits tests were carried out to examine the changes in the plasticity characteristics and shrinkage behavior of kaolin samples with increasing dosages of nano-materials (IS 2720 (Part 5), 1995; IS 2720 (Part 6), 1995). A hot-air oven maintained at 110±5°C was used for the determination of water content corresponding to the plasticity limits. The stress–strain curves obtained from unconfined compression strength (UCS) tests were used to ascertain the effect of treatment on strength development (IS 2720 (Part 10), 1995). The axial loading was applied to the specimen at a rate of 1.5 mm min–1 until failure. A proving ring with a 2.5 kN capacity and 0.0029 kN resolution was employed to measure the load during unconfined compression tests. The dial gauge used for deformation measurements typically has a precision of 0.01 mm. UCS tests were performed on samples at 7 and 28 days to assess the influence of curing time on strength attainment. Based on the plasticity and strength-test results, the optimum dosages of nano-materials, both $CaCO_3$ and silica, in kaolin were determined. Thereafter, clay treated with optimum dosages of nano-materials was subjected to consolidation tests. The conventional oedometer tests were performed to understand the changes in void ratio, rate of consolidation, and permeability characteristics of nano-treated specimens under increasing pressure (IS 2720 (Part 15), 1997). A dial gauge with a smallest unit of 0.002 mm was used for measuring the change in the height of the sample. After the application of final pressure, the samples were gradually unloaded in stages to evaluate the elastic or rebound characteristics of kaolin treated with nano-materials. Finally, the microstructural characterization study was conducted on nano-treated clay specimens using scanning electron microscopy (SEM), X-ray diffraction (XRD), Fourier-transform infrared spectroscopy (FTIR), and Brunauer-Emmett-Teller (BET) surface area analysis.

Field emission scanning electron microscopy (FESEM) was utilized to examine the nano-composite structure of the kaolin. The analysis was conducted in the SEM center at NIT Calicut, Kerala, India, using an Hitachi SU6600 variable pressure field emission scanning electron microscope. A 2–3 g sample of oven-dried, powdered kaolin after treatment with nano-materials of particle diameters <75 μm was coated with a thin layer of gold and spread evenly on an aluminum stub for analysis. The XRD test on treated clay samples was performed using the Bruker D8 Advance diffractometer facility at Sophisticated Analytical Instrument Facilities (SAIF) in Kochi. The powder XRD method used continuous step-scanning with a step size of 0.020°2θ in the range 10–80°2θ. FTIR spectra were obtained using a Jasco FT-IR spectrometer facility available at NIT Calicut, Kerala. The test specimens were prepared by mixing the dried clay samples with spectroscopic-grade potassium bromide (KBr) and then compressing the mixtures into pellet form. The scanning of samples was conducted across the spectral range of 4000–400 cm^{-1} with a resolution of 4 cm^{-1}. BET analysis was performed using a BELSORP-max with ultra-pure nitrogen adsorption at 77K to evaluate the porosity of kaolin after the treatment with nano-materials. The sample pre-treatment temperature was ~160°C.

Results and Discussion

Plasticity behavior

Plasticity is an important index property of clays. It is the ability of the clay to undergo deformation without cracking. Plastic limit is the water content at which clay loses its plasticity and passes to a

https://doi.org/10.1017/cmn.2025.1 Published online by Cambridge University Press

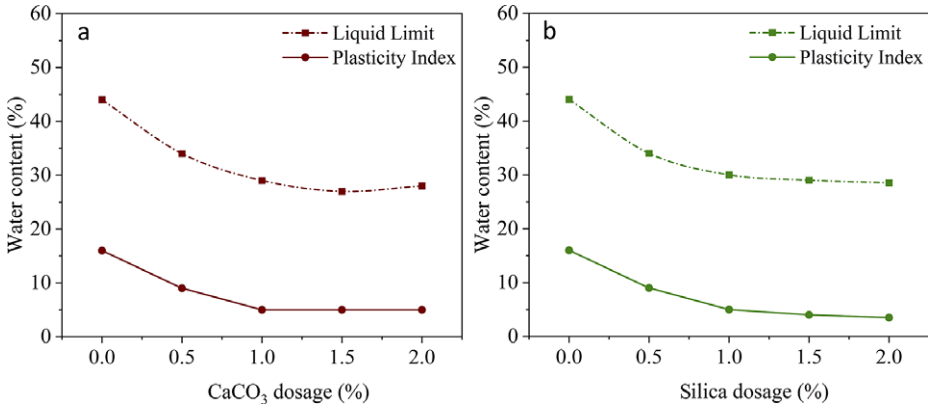


Figure 3. Variation of LL and PI in kaolin modified with: (A) calcium carbonate and (B) silica.

semi-solid state. Plasticity index is the difference between liquid limit and plastic limit. The consistency limits of kaolin mixed with varying proportions of either calcium carbonate or silica were determined (Fig. 3A,B). The LL and PI values decreased as the concentration of nano-materials increased. However, at higher dosages (>1%) of the nano-materials, both the LL and PI remained relatively constant.

The decrease in PI was due to the filling effect of nano-particles as well as cation exchange reactions between the kaolinite and calcium or silicate ions. The surface acidity played a critical role in the chemical reactions taking place at the interface of the kaolinite mineral and nano-material. The silica treatment increased soil alkalinity. At elevated pH levels, silica ions might have induced cation exchange reactions within the kaolin, resulting in reduced plasticity index. The grain-size distribution of kaolin was modified as nano-particles occupied the void spaces between the clay platelets. The incorporation of nano-materials elevated the clay pH from 7.8 to a range between 8.0 and 8.2. The greater pH increased the availability of exchangeable cations on both the edges and external basal surfaces of the mineral. The hydrogen ions of the exposed hydroxyls were replaced by calcium or silicon ions, resulting in a reduction in the thickness of the diffuse double layer. As a result, van der Waals attractive forces between the particles became dominant in the clay nano-composite matrix. Furthermore, the nano-size of the additives accelerated the cation exchange reactions (Ma and Eggleton, 1999).

The shrinkage limit (SL) of treated samples decreased with increasing concentration of nano-materials (Fig. 4). The relative grain-size distribution of the nano-composites improved with the inclusion of the nano-materials, resulting in a decreased shrinkage limit. Kaolin mostly exhibited a flocculated structure (Mietta et al., 2009). The filling of the voids with nano-particles reduced the water adsorption capacity of the clay, resulting in a lower shrinkage limit. The shrinkage limit was mainly influenced by the particle-packing phenomenon rather than by the plasticity characteristics. In general, the shrinkage limit decreases with decreasing particle size for low-plasticity clays (Sridharan and Prakash, 1998). Moreover, the spherical shape of silica particles facilitated denser particle packing in comparison with angular shaped calcium carbonate particles. The larger frictional properties of calcium particles provided greater resistance to shrinkage.

The shrinkage limit decreased gradually until reaching a 1% dosage of nano-materials, after which a significant reduction was observed. Up to 1% concentration, a portion of the nano-particles may have engaged in chemical reactions with the hydroxyl groups on the edge sites and external basal faces of kaolinite, and the remaining may have acted as filler material. Above 1%, excess amounts of nano-particles served as filler material because further chemical reactions were not initiated due to the minimal reactivity of kaolinite as a mineral. The increase in the proportion of finer fraction leads to a decreased shrinkage limit (Sridharan and Prakash, 1998).

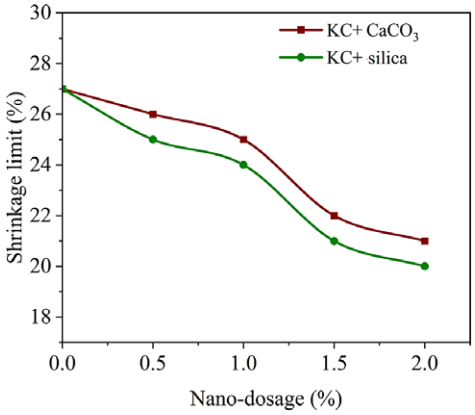


Figure 4. Variation of shrinkage limit in kaolin treated with $CaCO_3$ and silica.

Strength behavior

The unconfined compressive strength of kaolin mixed with varying percentages of $CaCO_3$ and silica at different curing periods (Figs 5 and 6) revealed a significant strength improvement when the kaolin was blended with nano-particles. The greatest strength was achieved in kaolin when mixed with 1% dosage of both nano-materials and, subsequently, a strength reduction was observed at 1.5% and 2% dosages. The unconfined strength of untreated kaolin was 180 kPa. This value increased to 345 and 435 kPa, respectively, with the addition of 1% of calcium carbonate and 1% of silica after a curing period of 7 days. Subsequently, after 28 days of curing, the strength was further improved to 450 and 550 kPa, respectively, with the incorporation of 1% of calcium carbonate or silica. Thus, 1% of nano-materials was the optimum dosage for the enhanced performance of kaolin.

The particulates of calcium carbonate and silica could act as good filler materials in kaolin. A similar observation was reported previously (Abhilash et al., 2021). The filling of voids by nano-particles densified the clay matrix, enhancing its capacity to support loads. The filling efficiency of nano-particles was affected remarkably by various factors

https://doi.org/10.1017/cmn.2025.1 Published online by Cambridge University Press

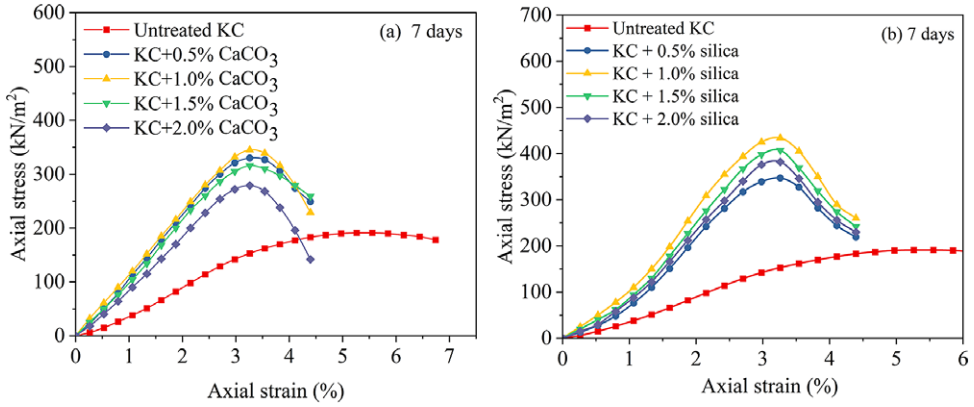


Figure 5. Stress–strain curves of 7-day cured kaolin modified using: (A) calcium carbonate and (B) silica.

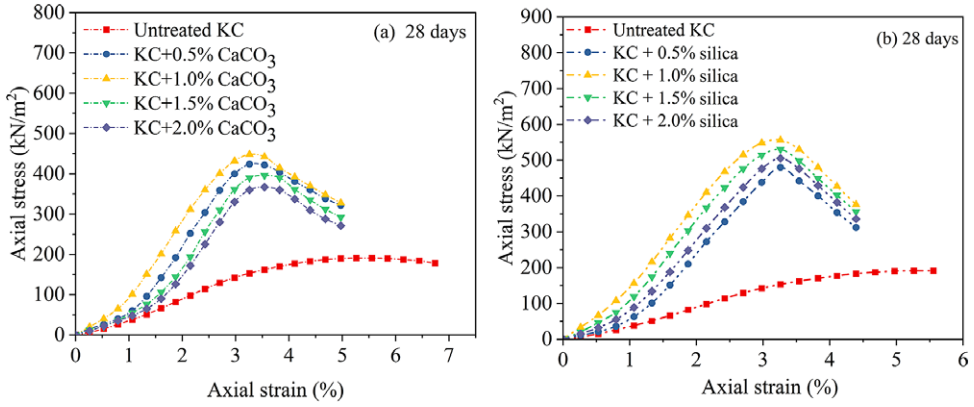


Figure 6. Stress–strain curves of 28-day cured kaolin modified using: (A) calcium carbonate and (B) silica.

such as the amount of filler used, the size and shape of the nano-particles, and their orientation within the material (Aksu and Eskisar, 2023). In the present study, the spherical shape and smaller size of silica ensured better packing within the clay matrix rather than with the addition of angular calcium carbonate particles.

In alkaline conditions (pH >7), the dissolution of silica and alumina from the clay lattice will take place at a greater rate. With the addition of calcium carbonate, calcium ions may have reacted with the silicate or aluminate ions within the kaolinite in the presence of inter-particle water content to form crystalline calcium silicate or calcium aluminate hydrate (CSH/CAH) gel. On the other hand, silica gel was generated with the addition of silica to kaolin. The silicate ions undergo a chemical reaction with the hydroxyl ions on the edge and external basal sites of the kaolinite ($O_{Si}\cdots H_{OH}$) or with the water adsorbed at the interface ($O_{Si}\cdots H_w$), resulting in the formation of the silica gel with strong hydrogen bonds (Sulpizi et al., 2012; Utama et al., 2018). The silicate ions may also react with some of the calcium ions present in kaolin (as given in XRF data) to form CSH gel. The presence of cementitious gel fostered interfacial molecular interactions encompassing electrostatic attraction, chemical bonding, and adsorption within the clay matrix, greatly enhancing its cohesive strength.

The strength of kaolin increased rapidly during the initial week of curing rather than after 4 weeks of curing. A similar trend in strength gain was reported by various researchers who worked with nano-materials (Land and Stephan, 2012; Abhilash et al., 2021). This could be attributed to the ability of nano-particles to initiate chemical reactions at an early age due to their large surface energy and nano-scale dimensions. The accelerated rate of reaction led to an earlier development of strength in the clay matrix. Strength at a later age may occur as a result of the prolonged effect of the pozzolanic reaction. The strength enhancement in kaolin also depends on the type of nano-material. Silica addition has been observed to be more effective in improving the strength of kaolin compared with that of calcium carbonate. This could be attributed to the following factors: (1) the smaller average size of silica nano-particles (30–50 nm) compared with calcium nano-particles (70–100 nm) could contribute to increased strength (Aksu and Eskisar, 2023); (2) the spherical shape of silica particles enabled denser packing compared with hexagonally shaped calcium particles; and (3) the hydrogen bonding in silica gel could potentially be stronger than that in CSH or CAH, further bolstering the overall strength of the kaolin nano-composite matrix.

The uniform dispersion of nano-materials in kaolin was difficult to achieve, especially at higher dosages of nano-materials. The nano-clay mixture may act as a rubber-like membrane, causing struggles in the preparation of test specimens. This could be one of the reasons for the lower strength of clay observed at 1.5% and 2% dosages. The self-agglomeration and more voids produced by the larger amount of nano-materials may result further in the loss of compressive strength. Similar nano-behavior was reported by several researchers (Kong et al., 2018; Abhilash et al., 2021). Excessive incorporation of nano-particles may encounter difficulties engaging in chemical reactions with kaolinite, owing to its low reactivity.

https://doi.org/10.1017/cmn.2025.1 Published online by Cambridge University Press

The breakdown and shifts of various peaks or changes in the basal spacings of XRD patterns (Fig. 7; see also Table S1 in the Supplementary material) confirmed the interaction of the kaolinite mineral with the nano-materials. The emergence of a new peak at 29.5°2θ (Fig. 7A) suggested the formation of calcium silicate hydrate (Choobbasti and Kutanaei, 2017). The changes in the intensities at 50 and 54.4°2θ also indicated the interaction of the clay mineral with the nano-material leading to the formation of calcium silicate hydrate (Maddalena et al., 2019; Madadi and Wei, 2022). The slight shift observed at 38.4°2θ suggested the generation of calcium aluminosilicate hydrate in kaolin modified with calcium carbonate (Morris, 1985; Veiga et al., 2020). The destruction of some peaks in the diffraction pattern as shown in Fig. 7B confirmed the structural interaction of clay platelets with silica. The relative changes in intensities exhibited at 26.7, 39.2, 45.5, and 73.6°2θ could represent the formation of silica gel in kaolin (Morris, 1981). The disappearance of the peak at 55°2θ was evidence for the formation of CSH gel resulting from the interaction between silicate ions in the nano-material and calcium ions in the kaolin.

Variations in the FTIR transmittance of different functional groups in the kaolin sample after treatment with nano-materials (Table 2; Fig. 8) revealed shifts in FTIR peaks as a result of the structural modifications in kaolin due to the addition of calcium carbonate and silica. The frequency of the bands in the range 3700–3600 cm^{-1} represents the surface hydroxyls (OH) of kaolinite (Kristóf et al., 1997), and the variations in frequency within this range suggested the generation of nano-crystalline calcium silicate hydrate gel and silica gel (Si–O–Si bonds) due to the interaction of nano-materials between the kaolinite layers (Lenza and Vasconcelos, 2001; Estrada-Flores et al., 2018). The variation of absorption peaks in the range of 2400 to 2000 cm^{-1} indicated both C=O stretching due to the carbonation of calcium silicate hydrate (CSH) gel (Lim and Mondal, 2015; Wu and Ye, 2016) and silica gel formation (Nayak and Bera, 2009). The FTIR band at 1120 cm^{-1} belonged to the Si–O stretching vibration of amorphous silica in the kaolinite mineral (Jozanikohan and Abarghooei, 2022). The FTIR peak at 1000 cm^{-1} corresponded to the Si–O bond, and the vibrations at this peak could point to the gelation caused by the structural deformation of Si–O–Si. The bending vibration of Al–OH was observed at 915 cm^{-1} (Lenza and Vasconcelos, 2001; Darmakkolla et al., 2016). The absorption spectra in the range 730–665 cm^{-1} indicated C=C bonding associated with CSH bonds (Jozanikohan and Abarghooei, 2022; Liu et al., 2023). The bending band found in the range 400–600 cm^{-1} represented the Si–O–Si bonds in silica tetrahedra of the kaolinite mineral, and the increase in vibrational frequency in this region suggested silica gel formation (Lenza and Vasconcelos, 2001; Thomas and Rangaswamy, 2020; Jozanikohan and Abarghooei, 2022). Based on the XRD and FTIR data, only small structural changes occurred in kaolinite following treatment with nano-materials. This confirmed the structural stability or low reactivity of kaolinite even after it interacts with nano-sized particles.

Table 2. FTIR peaks of kaolin before and after treatment with nanomaterials

Wavenumber (cm^{-1})	Transmittance (%)		
	Untreated KC	KC+1% $CaCO_3$	KC+1% silica
3819	92	89	95
3686	66	64	68
3618	59	57	62
2356	91	92	93
2168	92	94	96
2020	102	108	100
1727	96	101	99
1516	88	93	91
1294	92	98	95
1115	65	71	70
1024	12	14	16
997	5	8	6
909	14	15	17
905	14	16	18
791	73	67	74
668	72	58	71
549	23	18	38
527	9	6	19
423	14	2	4

Consolidation behavior

One-dimensional consolidation tests were performed to investigate the compressibility behavior of untreated and treated clay samples

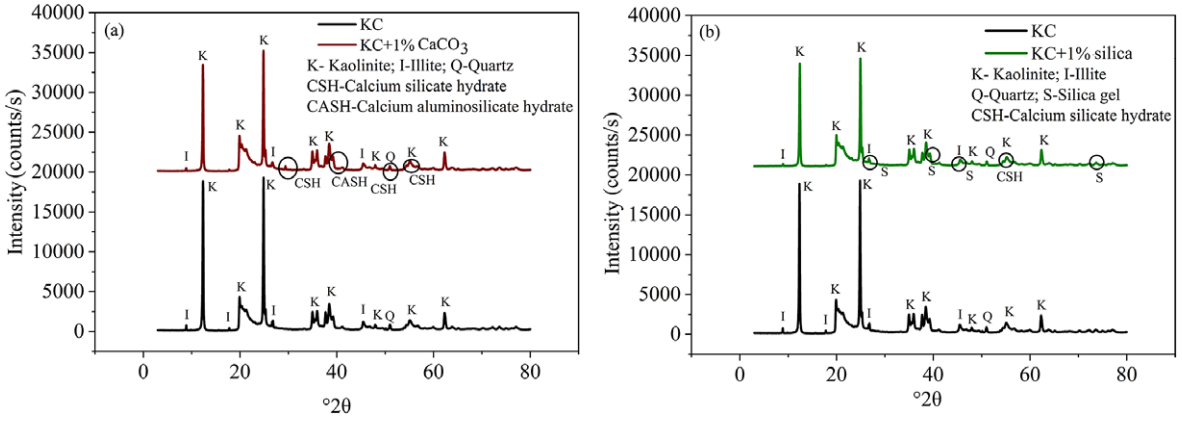


Figure 7. XRD patterns of kaolin modified with: (A) calcium carbonate and (B) silica.

https://doi.org/10.1017/cmn.2025.1 Published online by Cambridge University Press

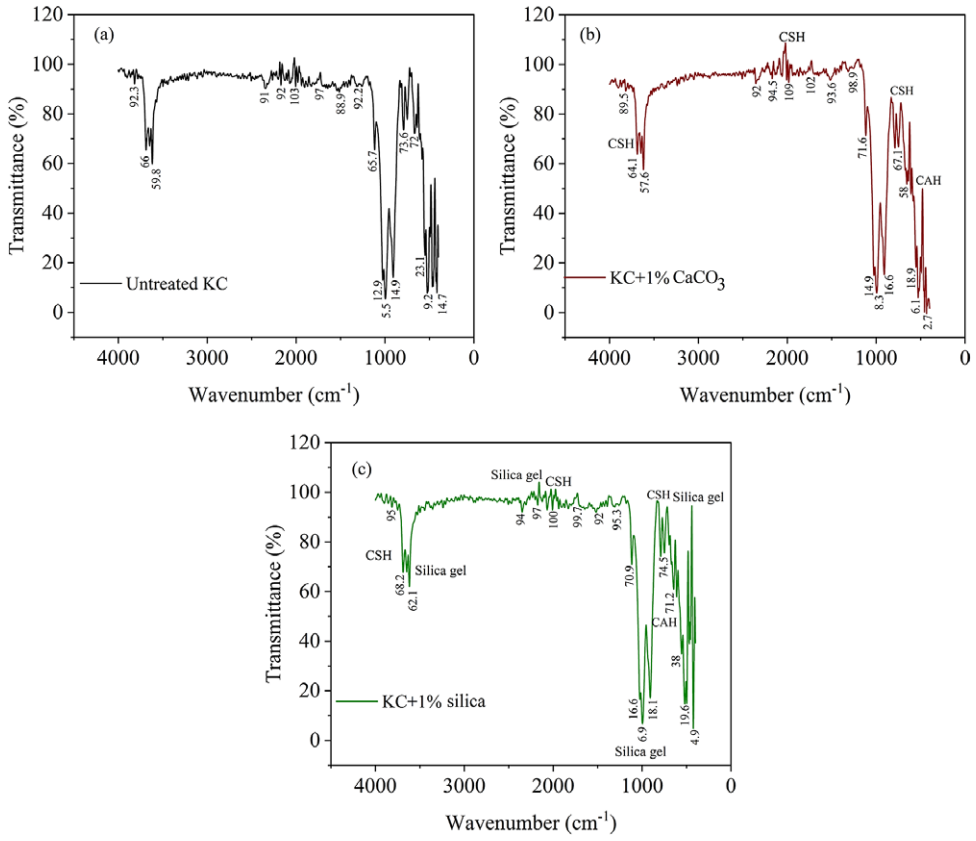


Figure 8. FTIR spectra of: (a) untreated KC; (b) KC treated with $CaCO_3$; and (c) KC treated with silica.

under the application of stress. The clay specimens, after treatment with the optimum doses of nano-materials and moisture content, and left for a curing period of 28 days, were compacted in the consolidation rings to their maximum dry density. The initial height and mass of the samples were measured. The entire assembly of the consolidation cell was mounted and positioned in the loading frame. The clay samples were then allowed to undergo saturation by connecting the base plate of the consolidation cell to a water reservoir. Initially, a seating stress of 6.25 kPa was applied to ensure the proper seating of the load and the cell alignment. The samples were loaded from 12.5 to 1600 kPa with a stress increment ratio of unity. Each load was left for ~24 h. After reaching the equilibrium state under 1600 kPa, the samples were unloaded in stages to the seating stress. Seating stress refers to a small amount of residual stress applied to a soil sample during loading and unloading in a consolidation or compression test. This stress is intentionally maintained to prevent the sample from losing contact with the loading apparatus, platen, or porous stones, ensuring the integrity of the test set-up. The samples were then dismantled from the consolidation frame for final measurements of mass and water content.

The void ratio–effective stress curves (Fig. 9) were plotted to ascertain the changes in the compressibility characteristics of the clay under vertical pressures after treatment. A significant parallel shift in the curves was noticed after introducing nano-particles into the kaolin. The void ratio increased upon blending the clay with the nano-materials, and the rate of increase was nearly the same for both additives. This illustrated a transition from microfabrics to nano-fabrics within the clay structure, potentially leading to the generation of numerous nano-perforations. However, the slope of the compression curves decreased, indicating a significant reduction in the compression index values of the clay with addition of nano-material. The compression index of kaolin decreased from 0.15 to 0.08 and 0.09, respectively, with calcium carbonate and silica treatment. This enhanced resistance to compressibility in kaolin may be due to the strong cementation effect facilitated by the CSH or silica gel. The improved elastic nature of the curves after modification using nano-materials was also revealed during the unloading stage.

Kaolinite crystals are typically thin layers or plates. The chemical interaction of nano-particles with the kaolinite caused surface distortions and refinement of the pore structure, leading to an

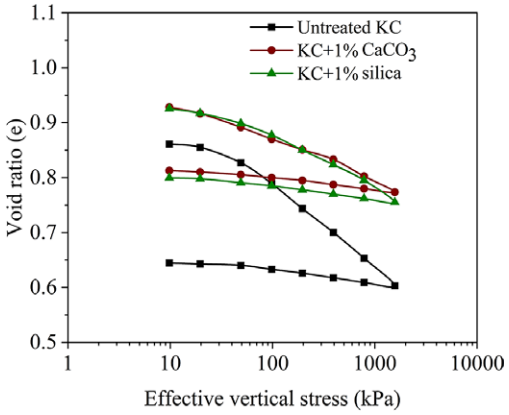


Figure 9. e-log σ curves of nano-treated kaolin.

https://doi.org/10.1017/cmn.2025.1 Published online by Cambridge University Press

increase in the void ratio of the clay nano-composite matrix (Maged et al., 2020). The calcium and silicate ions present in the additives may react chemically with the clay platelets leading to the formation of nano-crystalline CSH or silica gel. These gels bonded the clay platelets together, resulting in an aggregated-flocculated structure in the clay matrix with more void spaces.

When kaolin was modified with calcium carbonate particles, the clay platelets aggregated due to CSH gel formation, and subsequently underwent edge-to-face flocculation, resulting in a significant increase in the void spaces between them. On the other hand, in silica-modified clay, face-to-face associations of platelets were induced by silica gel, followed by flocculation with simultaneous development of distinct grain boundaries and pore spaces in the clay matrix. However, the silica-modified kaolin exhibited an apparent maximum packing fraction and a denser structure, which could explain its greater compressive yield stress capacity compared with clay treated with calcium carbonate particles. The enhanced porosity in kaolin after treatment is evident in the SEM images (Fig. 10).

Even though the pore volume increased with the addition of nanoparticles, the coefficient of permeability of the kaolin modified with nano-materials was more or less similar to that of untreated kaolin (10^{-9} to 10^{-12} m s^{-1}) under varying consolidation pressures (Fig. 11). The increase in void ratio due to the formation of an aggregated-flocculated structure did not affect the permeability of treated samples significantly, resulting in either a slight or no increase compared with that of untreated kaolin. The clay platelets aggregated due to nano-crystalline gel formation were rapidly and effectively bound together by bridging action, forming a strongly linked structure that hindered water movement through the pores. The SEM images revealed that the aggregated-flocculated fabric generated

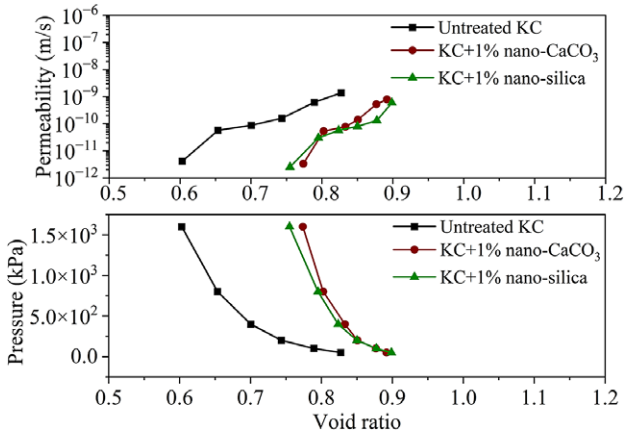


Figure 11. Permeability *versus* void ratio of nano-modified kaolin under varied consolidation pressures.

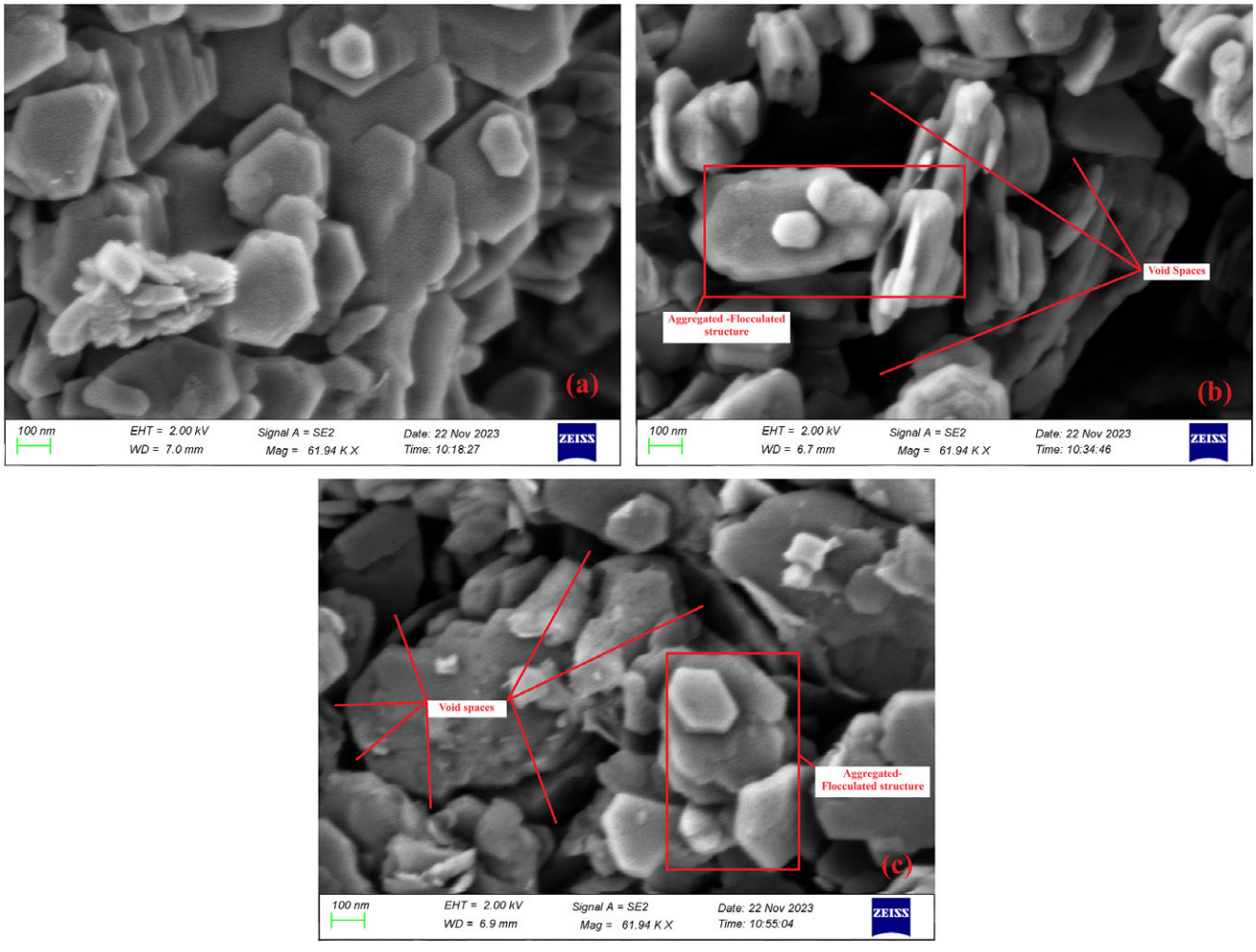


Figure 10. SEM images: (a) untreated KC, (b) calcium carbonate-modified KC and (c) silica-modified KC.

https://doi.org/10.1017/cmn.2025.1 Published online by Cambridge University Press

closed loops within the clay nano-composite matrix. The poor connectivity of pores could create barriers to fluid movement, and as a result, no significant improvement in the rate of consolidation was noticed in clays modified with nano-materials. Furthermore, path tortuosity induced by nano-perforations might slow down the fluid flow and impede permeability.

Brunauer-Emmett-Teller (BET) analysis was performed on kaolin before and after treatment, which could give more insights into the pore-size distribution. The total pore volume of kaolin increased from 0.043 to 0.068 $cm^3\ g^{-1}$ and 0.063 $cm^3\ g^{-1}$ after treatment with calcium carbonate and silica, respectively. In addition, the average pore diameter of the clay matrix increased from 16.04 to 27.46 nm and 18.07 nm following the treatments with calcium carbonate and silica, respectively.

Conclusions

The extensive testing program conducted on nano-treated kaolin led to the following conclusions:

(1) The decrease in the plasticity index values of kaolin when treated with nano-materials can be ascribed to the filling effect of nano-particles and the cation exchange reactions between the mineral and calcium or silicate ions present in the nano-materials. The addition of nano-particles resulted in the particle-size rearrangement of kaolin and reduced the shrinkage limit values.
(2) The unconfined compressive strength of kaolin was increased by ×2.5 and ×3, respectively, with the incorporation of 1% calcium carbonate and 1% silica after a curing age of 28 days. Kaolin exhibited better performance and a significant strength enhancement when treated with silica particles compared with calcium carbonate treatment.
(3) The compressibility of kaolin was reduced to almost half after treatment. This may be due to the development of strong linked structures that resulted from the cementation effects induced by the nanocrystalline calcium silicate hydrate or calcium aluminate hydrate gel and silica gel. The treatment using nano-materials increased the porosity of the clay matrix. However, the permeability was little affected due to the increased grain boundaries, which could hinder the fluid flow.
(4) The XRD pattern, FTIR spectra, SEM images, and BET analysis results confirmed the nanocrystalline gel formation within the clay nanocomposite matrix.

Supplementary material. The supplementary material for this article can be found at http://doi.org/10.1017/cmn.2025.1.

Author contributions. Swapna Thomas: experimental investigation, original draft preparation; S. Chandrakaran: conceptualization, supervision; N. Sankar: methodology, visualization.

Acknowledgements. The authors thank the Department of Science and Technology (DST), Government of India, and SEM Centre, Department of Materials Science and Engineering, National Institute of Technology Calicut, for providing the facility purchased under the scheme 'Fund for Improvement of Science and Technology' (FIST – No. SR/FST/ET-I/2021/840) during the period of the present research work.

Financial support. This research did not receive any specific grant from funding agencies in the public, commercial, or private sectors.

Competing interests. The authors have no competing interests to declare that are relevant to the content of this article.

Data availability statement. The authors confirm that the data supporting the findings of this study are available within the article.

References

Abhilash, P.P., Nayak, D.K., Sangoju, B., Kumar, R., & Kumar, V. (2021). Effect of nano-silica in concrete; a review. *Construction and Building Materials*, *278*, 122347. https://doi.org/10.1016/j.conbuildmat.2021.122347

Aksu, G., & Eskisar, T. (2023). The geomechanical properties of soils treated with nanosilica particles. *Journal of Rock Mechanics and Geotechnical Engineering*, *15*, 954–969. https://doi.org/10.1016/j.jrmge.2022.06.013

Aziz, M., Hamza, M., Rasool, A.M., Ali, U., Ahmed, T., Kharal, Z.N., Khan, A.H., & ur Rehman, Z. (2023). Use of graphene oxide nanomaterial to improve mechanical properties of cement-treated silty soil. *Arabian Journal for Science and Engineering*, *48*, 5603–5618. https://doi.org/10.1007/s13369-022-07530-w

Cheng, H., Liu, Q., Yang, J., Ma, S., & Frost, R.L. (2012). The thermal behavior of kaolinite intercalation complexes – a review. *Thermochimica Acta*, *545*, 1–13. https://doi.org/10.1016/j.tca.2012.04.005

Choobbasti, A. J., & Kutanaei, S. S. (2017). Microstructure characteristics of cement-stabilized sandy soil using nanosilica. *Journal of Rock Mechanics and Geotechnical Engineering*, *9*, 981–988. https://doi.org/10.1016/j.jrmge.2017.03.015

Darmakkolla, S.R., Tran, H., Gupta, A., & Rananavare, S.B. (2016). A method to derivatize surface silanol groups to Si-alkyl groups in carbon-doped silicon oxides. *RSC Advances*, *6*, 93219–93230. https://doi.org/10.1039/c6ra20355h

Estrada-Flores, S., Martínez-Luévanos, A., Bartolo-Pérez, P., García-Cerda, L. A., Flores-Guia, T.E., & Aguilera-González, E.N. (2018). Facile synthesis of novel calcium silicate hydrated-nylon 6/66 nanocomposites by solution mixing method. *RSC Advances*, *8*, 41818–41827. https://doi.org/10.1039/c8ra07116k

Fattahi Masrour, F., Naghdipour Mirsadeghi, M., MolaAbasi, H., & Jamshidi Chenari, R. (2021). Effect of nanosilica on the macro- and microbehavior of dispersive clays. *Journal of Materials in Civil Engineering*, *33*, 04021349. https://doi.org/10.1061/(asce)mt.1943-5533.0003975

Harman, C.G., & Fraulini, F. (1940). Properties of kaolinite as a function of its particle size. *Journal of the American Ceramic Society*, *23*, 252–259. https://doi.org/10.1111/j.1151-2916.1940.tb14271.x

IS 1498 (1970). *Classification and Identification of Soils for General Engineering Purposes.*

IS 2720 (Part 10) (1995). *Methods of Test for Soils: Detrmination of Unconfined Compressive Strength.*

IS 2720 (Part 15) (1997). *Methods of Test for Soils: Determination of Consolidation Properties.*

IS 2720 (Part 5) (1995). *Methods of Test for Soils: Determination of Liquid and Plastic limit.*

IS 2720 (Part 6) (1995). *Methods of Test for Soils: Determination of Shrinkage Factors.*

IS 2720 (Part 7) (1997). *Methods of Test for Soils: Determination of Water Content–Dry Density Relation Using Light Compaction.*

Jozanikohan, G., & Abarghooei, M.N. (2022). The Fourier transform infrared spectroscopy (FTIR) analysis for the clay mineralogy studies in a clastic reservoir. *Journal of Petroleum Exploration and Production Technology*, *12*, 2093–2106. https://doi.org/10.1007/s13202-021-01449-y

Kannan, G., & Sujatha, E.R. (2021). A review on the choice of nano-silica as soil stabilizer. *Silicon.* https://doi.org/10.1007/s12633-021-01455-z

Karimiazar, J., Sharifi Teshnizi, E., Mirzababaei, M., Mahdad, M., & Arjmandzadeh, R. (2022). California Bearing Ratio of a reactive clay treated with nano-additives and cement. *Journal of Materials in Civil Engineering*, *34*, 04021431. https://doi.org/10.1061/(asce)mt.1943-5533.0004028

Kong, R., Zhang, F., Wang, G., & Peng, J. (2018). Stabilization of loess using nano-SiO_2. *Materials*, *11*, 1–14. https://doi.org/10.3390/ma11061014

Kristóf, J., Frost, R.L., Felinger, A., & Mink, J. (1997). FTIR spectroscopic study of intercalated kaolinite. *Journal of Molecular Structure*, *410–411*, 119–122. https://doi.org/10.1016/S0022-2860(96)09488-4

Land, G., & Stephan, D. (2012). The influence of nano-silica on the hydration of ordinary Portland cement. *Journal of Materials Science*, *47*, 1011–1017. https://doi.org/10.1007/s10853-011-5881-1

Lenza, R.F.S., & Vasconcelos, W.L. (2001). Preparation of silica by sol-gel method using formamide. *Materials Research*, *4*, 189–194.

Lim, S., & Mondal, P. (2015). Effects of incorporating nanosilica on carbonation of cement paste. *Journal of Materials Science*, *50*, 3531–3540. https://doi.org/10.1007/s10853-015-8910-7

Liu, C.H., Ghadr, S., Mrudunayani, P., & Hung, C. (2023). Synergistic effects of colloidal nanosilica and fiber on the hydromechanical performance of mudstone soil in Taiwan. *Acta Geotechnica*, *18*, 6831–6847. https://doi.org/10.1007/s11440-023-01969-3

Ma, C.H.I., & Eggleton, R.A. (1999). Cation exchange capacity of kaolinite. *Clays and Clay Minerals*, *47*, 174–180.

Madadi, A., & Wei, J. (2022). Characterization of calcium silicate hydrate gels with different calcium to silica ratios and polymer modifications. *Gels*, *8*, 1–17. https://doi.org/10.3390/gels8020075

Maddalena, R., Li, K., Chater, P.A., Michalik, S., & Hamilton, A. (2019). Direct synthesis of a solid calcium-silicate-hydrate (C-S-H). *Construction and Building Materials*, *223*, 554–565. https://doi.org/10.1016/j.conbuildmat.2019.06.024

Maged, A., Ismael, I.S., Kharbish, S., Sarkar, B., Peräniemi, S., & Bhatnagar, A. (2020). Enhanced interlayer trapping of Pb(II) ions within kaolinite layers: intercalation, characterization, and sorption studies. *Environmental Science and Pollution Research*, *27*, 1870–1887. https://doi.org/10.1007/s11356-019-06845-w

Meng, T., Qiang, Y., Hu, A., Xu, C., & Lin, L. (2017). Effect of compound nano-$CaCO_3$ addition on strength development and microstructure of cement-stabilized soil in the marine environment. *Construction and Building Materials*, *151*, 775–781. https://doi.org/10.1016/j.conbuildmat.2017.06.016

Mietta, F., Chassagne, C., & Winterwerp, J.C. (2009). Shear-induced flocculation of a suspension of kaolinite as function of pH and salt concentration. *Journal of Colloid and Interface Science*, *336*, 134–141. https://doi.org/10.1016/j.jcis.2009.03.044

Miranda-Trevino, J.C., & Coles, C.A. (2003). Kaolinite properties, structure and influence of metal retention on pH. *Applied Clay Science*, *23*, 133–139. https://doi.org/10.1016/S0169-1317(03)00095-4

Mitchell, J.K., & Soga, K. (1994). *Fundamentals of Soil Behavior*. John Wiley & Sons. https://doi.org/10.1097/00010694-199407000-00009

Moayed, R.Z., & Rahmani, H. (2017). Effect of nano-SiO_2 solution on the strength characteristics of kaolinite. *International Journal of Environmental, Chemical, Ecological, Geological and Geophysical Engineering*, *11*, 83–87.

Mohammadi, M., Khodaparast, M., & Rajabi, A.M. (2022). Effect of nano calcium carbonate (nano $CaCO_3$) on the strength and consolidation properties of clayey sand soil. *Road Materials and Pavement Design*, *23*, 2394–2415. https://doi.org/10.1080/14680629.2021.1976255

Morris, M.C. (1981). *Standard X-ray Diffraction Powder Patterns Section 18*. National Bureau of Standards.

Morris, M.C. (1985). *Standard X-ray Diffraction Powder Patterns Section 21*. National Bureau of Standards.

Naseri, F., Irani, M., & Dehkhodarajabi, M. (2016). Effect of graphene oxide nanosheets on the geotechnical properties of cemented silty soil. *Archives of Civil and Mechanical Engineering*, *16*, 695–701. https://doi.org/10.1016/j.acme.2016.04.008

Nayak, J., & Bera, J. (2009). A simple method for production of humidity indicating silica gel from rice husk ash. *Journal of Metals, Materials and Minerals*, *19*, 15–19. http://jmmm.material.chula.ac.th/index.php/jmmm/article/view/230

Parsaei, M., Rojhani, M., & Seyedahmadian, S. (2023). Effect of the addition of nano alumina on the mechanical properties of clay. *Geotechnical and Geological Engineering*, *41*, 3767–3779. https://doi.org/10.1007/s10706-023-02488-4

Sridharan, A., & Prakash, K. (1998). Mechanism controlling the shrinkage limit of soils. *Geotechnical Testing Journal*, *21*, 240–250. https://doi.org/10.1520/gtj10897j

Sulpizi, M., Gaigeot, M.P., & Sprik, M. (2012). The silica5–water interface: how the silanols determine the surface acidity and modulate the water properties. *Journal of Chemical Theory and Computation*, *8*, 1037–1047. https://doi.org/10.1021/ct2007154

Thomas, G., & Rangaswamy, K. (2020). Strengthening of cement blended soft clay with nano-silica particles. *Geomechanics and Engineering*, *20*, 505–516. https://doi.org/10.12989/gae.2020.20.6.505

Thomas, S., Chandrakaran, S., & Sankar, N. (2022). Nanocomposites are state-of-the-art in the field of ground improvement- a review. *Materials Today: Proceedings*, *65*, 877–882. https://doi.org/10.1016/j.matpr.2022.03.454

Thomas, S., Chandrakaran, S., & Sankar, N. (2023). Effect of nano-calcium carbonate on the geotechnical and microstructural characteristics of highly plastic paddy clay. *Arabian Journal for Science and Engineering*, *48*, 12977–12989. https://doi.org/10.1007/s13369-023-07679-y

Thomas, S., Chandrakaran, S., & Sankar, N. (2024). Role of nano-silica additive on the strength behaviour of a highly plastic clay found in an Indian paddy field. *Indian Geotechnical Journal*, 0123456789. https://doi.org/10.1007/s40098-024-00945-2

Utama, P.S., Yamsaensung, R., & Sangwichien, C. (2018). Silica gel derived from palm oil mill fly ash. *Songklanakarin Journal of Science and Technology*, *40*, 121–126. https://doi.org/10.14456/sjst-psu.2018.27

Veiga, F.C.T., González, R.F., Egea, J.J., da Silva Cava, S., & de Sousa, V.C. (2020). Mixed electrical conduction of calcium aluminates synthesized by polymeric precursors. *Materials Research*, *22*, 1–12. https://doi.org/10.1590/1980-5373-MR-2018-0271

Wu, B., & Ye, G. (2016). Carbonation mechanism of different kind of C-S-H: rate and products. *Concrete with Supplementary Cementitious Materials*, 263–272. https://biblio.ugent.be/publication/8531148

Zhou, G.X., Zhong, J., Zhang, H., Hu, X., Wu, J., Koratkar, N., & Shi, X. (2017). Influence of releasing graphene oxide into a clayey sand: physical and mechanical properties. *RSC Advances*, *7*, 18060–18067. https://doi.org/10.1039/c7ra01539a

https://doi.org/10.1017/cmn.2025.1 Published online by Cambridge University Press